

Pascal A. T. Baltzer
Tibor Vag
Matthias Dietzel
Sebastian Beger
Christian Freiberg
Mieczyslaw Gajda
Oumar Camara
Werner A. Kaiser

Computer-aided interpretation of dynamic magnetic resonance imaging reflects histopathology of invasive breast cancer

Received: 22 October 2009
Accepted: 14 December 2009
Published online: 4 March 2010
© European Society of Radiology 2010

P. A. T. Baltzer (✉) · T. Vag ·
M. Dietzel · S. Beger · C. Freiberg ·
W. A. Kaiser
Institute of Diagnostic and
Interventional Radiology,
Friedrich Schiller University of Jena,
Erlanger Allee 101,
07740 Jena, Germany
e-mail: pascal.baltzer@med.uni-jena.de
Tel.: +49-3641-9324974
Fax: +49-3641-9324832

M. Gajda
Institute of Pathology,
Friedrich Schiller University of Jena,
Ziegmühlenweg 1,
07740 Jena, Germany

O. Camara
Clinic of Gynecology,
Friedrich Schiller University of Jena,
Bachstr. 18,
07740 Jena, Germany

Abstract Objective: To perform a semiautomated software-based comparison of invasive breast carcinoma dynamic enhancement patterns in MR mammography with histological prognostic factors considering whole lesion volumes. *Material and methods:* A total of 128 patients with 145 invasive breast carcinomas underwent dynamic MR mammography. Kinetic features from the invasive breast lesions were obtained using commercially available software to automatically assess volume enhancement characteristics of a manually chosen lesion. Findings were compared with histological factors determining tumour aggressiveness (lymph node status, LN; oestrogen/progesterone receptor (ER/PR) status; HER-2/neu status; tumour grade) by using nonparametric rank tests and binary logistic regression analysis (BLRA). *Results:* Volume enhancement characteristics were significantly influenced by LN, ER/PR and HER-

2/neu status ($P < 0.05$). BLRA implied that total lesion and plateau voxel volume were independent predictors of ER/PR and HER-2/neu status. Strongest initial enhancement predicted negative ER/PR, and time to peak of the most suspect curve was inversely correlated with positive LN status. On the other hand, no statistical significance could be observed between histological tumour grading and kinetic features. *Conclusion:* Histopathological criteria associated with poor prognosis lead to significantly more aggressive dynamic enhancement patterns in MR mammography. In this study, higher lesion volumes as well as higher and earlier initial enhancement were independent covariates predicting higher tumour aggressiveness.

Keywords Breast · Neoplasm · MRI · DCE-MRI · Computer-assisted diagnosis

Introduction

Dynamic contrast enhanced magnetic resonance mammography (MRM) is a well-established method in the diagnosis of invasive breast cancer with a sensitivity near 100% [1–4]. Distinction between benign and malignant lesions in MRM is possible by evaluating their morphology and enhancement pattern [5–8]. A strong initial signal increase followed by a plateau or washout curve is regarded as indicative of malignancy, whereas a slow initial enhancement and a persistent curve type are thought to be

associated with benign lesions. However, overlapping enhancement features exist, corroborating the need for additional morphological descriptors for differential diagnosis of breast lesions. The overlap of kinetic features with benign lesions is especially distinct in less aggressive, noninvasive cancers [9]. As contrast enhancement is thought to reflect tumour angiogenesis, several studies have investigated whether MRI kinetic lesion features correlate with established prognostic histopathological factors of invasive breast cancer. Such knowledge would help to improve tumour classification regarding possible

therapeutic pathways. Results of previous investigations varied significantly with some authors confirming such correlation [10–12], while other authors could not find any association between MRI enhancement features and pathologic prognostic factors [4, 13].

In this study, we assessed the kinetic profile of invasive breast lesions by using computer-aided evaluation software to exclude interobserver variability. Furthermore, such software is able to deliver additional information about the enhancement pattern of the whole tumour volume, which cannot be assessed by manual analysis [14]. The hypothesis (H^1) was that a significant difference in the kinetic lesion profile depended on prognostic histopathological factors (tumour grade, expression of hormone receptors, HER-2/neu antigen and lymph node status).

Material and methods

Patients and lesion workup

Institutional review board approval was obtained for this prospective study of previously acquired examinations. Between January 2005 and October 2006, all patients with complete histopathology workup of invasive carcinomas at our university hospital were identified among 1,109 examinations performed at our department. Only the largest lesion per cancer-bearing breast (reference lesion) was rated in cases of multifocal disease in order to eliminate biological bias. Exclusion criteria were chemotherapy or interventions prior to the MR examination. All patients underwent vacuum biopsy and subsequent surgery or open surgery primarily. Histopathology diagnosis was established by open surgery in all lesions. Routine pathologic assessment by board certified breast pathologists included lymph node status (LN), oestrogen/progesterone receptor (ER/PR) status, HER-2/neu expression and tumour grading.

MRI technique

All MR images were obtained on clinical 1.5-T MRI systems (a 1.5-T Symphony from Siemens Medical Solutions, Erlangen, Germany) using a dedicated phased array double breast coil with the patient in prone position. For the dynamic study, a multi-slice T1-weighted (T1w) spoiled gradient echo sequence (FLASH 2D) in axial orientation was obtained by using the following parameters: GRAPPA factor 2, repetition time 113 ms, echo time 5 ms, flip angle 80°, spatial resolution 1.1×0.9×3 mm, 33 slices). Following the acquisition of the native T1w images, 0.1 mmol/kg per body weight gadopentetate dimeglumine (Magnevist, Bayer Healthcare, Germany) was intravenously administered as a rapid bolus at 3 ml/s, followed by a saline flush of 20 ml. Thirty seconds after the

beginning of the contrast material administration, dynamic MR data acquisition was continued with the same sequence parameters and under identical tuning conditions at 1-min intervals up to 7 min after contrast material administration. Unenhanced images were automatically subtracted from enhanced dynamic images. After dynamic MR imaging, axial T2-weighted turbo spin echo images (GRAPPA factor 2, TR 8,900 ms, TE 207 ms, flip angle 90°, spatial resolution 0.8×0.7×3 mm, 33 slices) and an axial turbo spin echo inversion recovery (TIRM) sequence with magnitude reconstruction (GRAPPA factor 2, TR 8,420 ms, TE 70 ms, TI 150 ms, flip angle 180°, spatial resolution 1.7×1.4×3 mm, 33 slices) were obtained in identical slice positions.

Computer analysis

All collected data were processed by using computer-aided evaluation software (DynaCAD Invivo, USA). All analyses were performed in consensus by two observers trained in handling the program. DynaCAD incorporates the unenhanced and enhanced T1w MRM series and calculates an enhancement curve for each pixel in a user-specified volume of interest (VOI) by comparing values of the unenhanced and the enhanced series. If the pixel value between the unenhanced and the first enhanced series increases by a determined threshold, the pixel will be shown in colour on the MR image. We set the initial threshold (first measurement after contrast material injection) to 50%, which resembles the standard region of interest (ROI) procedure in our clinical routine using the given sequence parameters and contrast material dosage (cf. Figs. 1 and 2). A second threshold for strong initial enhancement was set to 100%. Lesion parts not passing the 50% threshold were not colour-coded and were thus not analysed by the system. Delayed phase enhancement is defined by subtraction of enhancement values of the last time point (450 s after injection of contrast material) from the first time point after injection of contrast material (90 s). A signal decrease of more than 10% is defined as washout (cf. Fig. 1c). On the other hand, signal increase by more than 10% is defined as persistent enhancement pattern. If a pixel value does not change in either direction by more than 10%, enhancement pattern is classified as plateau. The percentages of regions demonstrating different enhancement curves in a given lesion are automatically summarized in an enhancement profile of the lesion by the program (cf. Fig. 1d). The following kinetic profile descriptors were extracted and analysed: total colour-coded volume (in ccm), percentage of persistent, plateau and washout voxels within a lesion, and percentage of initially strong (above 100%) enhancing voxels. Curve type volumes were calculated by multiplication of curve type voxel percentages by total colour-coded volume. Furthermore, the computer system automatically detected the most suspect

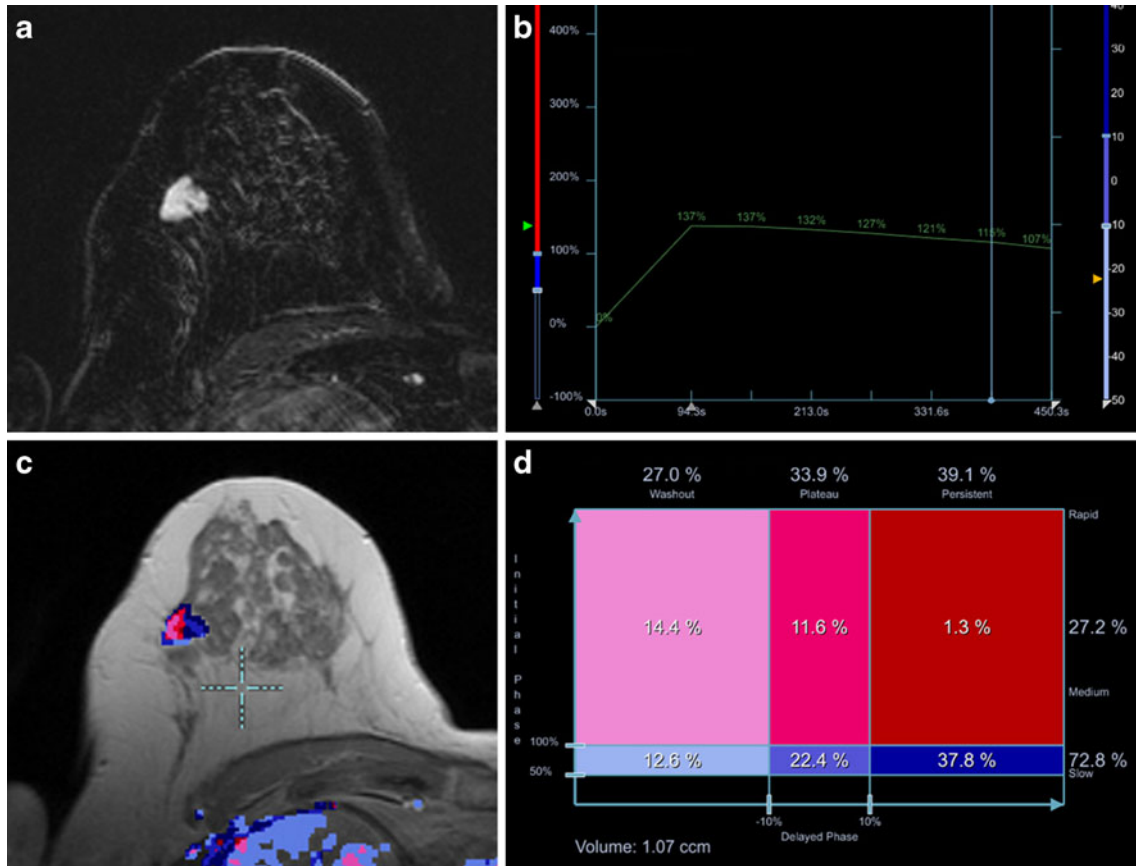
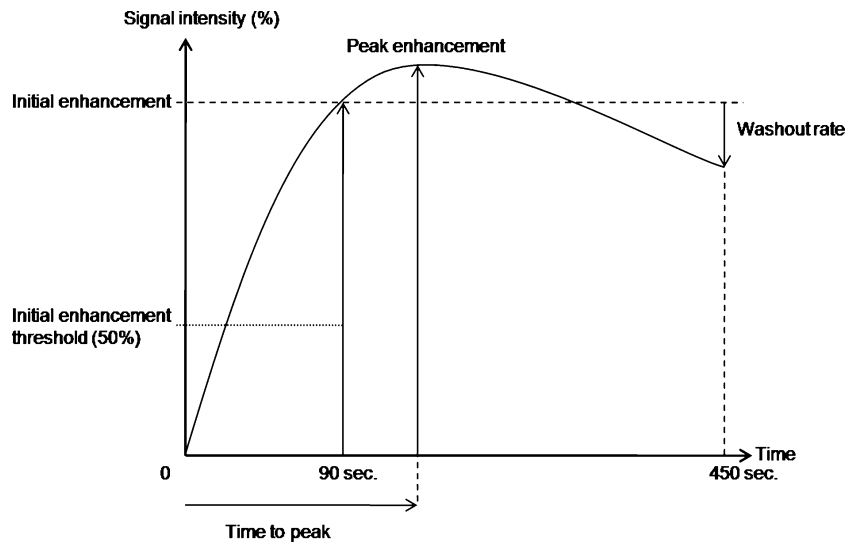


Fig. 1 A 75-year-old female patient with invasive ductal cancer G3, size 13 mm, ER+, PR-, HER-2/neu-, LN+. Subtraction image, first minute after contrast agent injection shows strong and irregular enhancing mass in the right breast (a). Computer-assisted diagnosis (CAD) results of dynamic analysis are displayed as a colour-coded

parametric map (b). Quantitative CAD analysis reveals the most suspect curve with strong initial enhancement with peak enhancement after the first minute, followed by strong washout (c). Curve type percentages for each colour-coded voxel as well as lesion volume is given in (d)

Fig. 2 Diagram illustrating the characteristics used for analysis of the most suspect curve. Initial enhancement is measured after the first postcontrast measurement (i.e. 90 s). Washout rate is calculated by subtraction of signal intensity at the last time point (i.e. 450 s) from signal intensity at the first time point. Voxels not passing the threshold for initial enhancement (i.e. 50%) were omitted by the computer analysis



enhancement pattern (curve type) within a lesion, defined by the highest initial enhancement to highest washout rate. The most suspect curve characteristics analysed were (cf. Fig. 2): initial enhancement percentage (first enhanced measurement), washout rate (subtraction of last from first enhanced signal intensity percentage), maximum enhancement rate (the maximum enhanced signal increase) and the time to peak (time from contrast agent injection to maximum enhancement rate). Lesions failing to exceed the initial enhancement threshold were omitted, since the purpose of the study was to correlate dynamic features with prognostic factors of breast lesions rather than assessing the diagnostic accuracy (sensitivity and specificity) of the program.

Histopathological analysis

Histopathological examinations were performed by board certified breast pathologists according to the TNM classification. Lymph nodes were assessed by using the sentinel method. If lymph nodes were positive either clinically or pathologically, axillary node dissection was carried out. Antibody stainings for the standardized assessment of additional prognostic factors were performed by using formaldehyde-fixed, deparaffinised tissue sections. Specific staining of oestrogen receptors (ER), progesterone receptors (PR) and HER-2/neu was performed by using a standardized protocol. The primary antibodies used for immunohistochemical staining were: Dako Monoclonal Mouse Anti Human Oestrogen Receptor α Clone 1D5, PR Dako Monoclonal Mouse Anti Human Progesterone Receptor Clone PgR 636 and Hercept TestTM for the Dako Autostainer Code K 5207. Staining for ER, PR and HER-2/neu was assessed by counting the percentage of stained cancer cells in the invasive part of the tumour.

Statistics

SPSS for Windows 15.0 was used for statistical analysis. For statistical analysis, pathological ratings were dichotomized according to the following clinical thresholds: hormone receptors (ER, PR) $\leq 10\%$ (negative), $>10\%$ (positive); HER-2/neu 0–2 (negative), 3+ (positive). Lymph node status could be either positive (any N except N0) or negative (N0). Exact nonparametric rank tests (two-sided Mann–Whitney *U* test for dichotomized, Kruskal–Wallis test for not dichotomized variables, i.e. grading) were performed to test the H^1 hypothesis on differences between kinetic profiles and histopathological variables. Normal distribution was excluded by calculation of kurtosis and skewness. *P* values smaller 0.05 were regarded as evidence for a relationship or difference between the factors analysed, whereas *P* values between 0.1 and 0.05 were regarded as weak evidence for a difference or relationship between the factors analysed.

In order to identify independent predictor variables, computer-measured dynamic parameters with significant differences between pathological prognostic factors in univariate analysis were further analysed by binary logistic regression using backward feature elimination on the basis of likelihood ratios. Histopathological criteria were used as dependent variables and dynamic enhancement parameters as covariates. Probabilities of 0.05 and 0.1 were chosen as enter and remove limits for covariates in the regression model.

Results

Patients and lesions

A total of 159 lesions in 142 patients were primarily identified, of which 14 lesions in 14 patients did not pass the initial enhancement threshold of the computer-aided evaluation software used and were thus omitted. As a result, a cohort of 128 patients (age range 30–82 years, mean 60 years) with 145 invasive cancer lesions was included in this study. Out of these, 125 lesions proved to be of invasive ductal, 12 lesions of invasive lobular and 8 lesions of mucinous origin.

Lesion features and lymph node status

Forty-five lesions proved to have metastasized (positive) lymph nodes at histopathology, whereas 100 lesions demonstrated negative lymph nodes. Lesions with positive lymph nodes had a significantly ($P=0.002$) larger tumour volume (median 1.72, interquartile range 3.04 ccm) compared with lesions without metastasized lymph nodes (median 0.78, interquartile range 2.6 ccm). Significant higher persistent and plateau voxel volumes were found in lymph node positive tumours ($P=0.007$ and $P=0.003$, respectively), whereas washout voxel volume only tended to be higher in lymph node positive cases ($P=0.085$). Time to peak of the most suspect curve was shorter in lymph node positive tumours compared with lymph node negative cases ($P=0.043$).

The other dynamic features examined showed no significant differences between lymph node positive and lymph node negative lesions (cf. Tables 1 and 2).

Binary logistic regression analysis identified only time to peak of the most suspect curve as an independent predictor for lymph node status (cf. Table 3).

Lesion features and HER-2/neu score

A total of 102 lesions showed a HER-2/neu score of 0–2 and were regarded as negative, whereas 43 lesions showed a HER-2/neu score of 3+ and were counted as positive. At a weak evidence level ($P=0.076$), HER-2/neu positive

Table 1 Prognostic pathological factors and characteristics of the most suspect curve

Prognostic factor	Initial enhancement (median %)	Washout rate (median %)	Peak enhancement (median %)	Time to peak (min)
LN- (<i>n</i> =100)	113.0 (36.8)	26.0 (33.5)	118.0 (29.5)	1 (2)
LN+ (<i>n</i> =45)	115.0 (44.0)	25.0 (29.5)	116 (39.5)	1 (1)
<i>P</i> value	0.841	0.508	0.739	0.043**
HER-2- (<i>n</i> =102)	113.5 (42.3)	26.0 (33.3)	118.0 (35.8)	1 (1)
HER-2+ (<i>n</i> =43)	113.0 (34.0)	26.0 (23.0)	119.0 (33.0)	1 (1)
<i>P</i> value	0.686	0.608	0.975	0.146
ER- (<i>n</i> =41)	120.0 (32.5)	34.0 (39.5)	122.0 (34.0)	1 (1)
ER+ (<i>n</i> =104)	112.0 (39.8)	25.0 (25.5)	116.0 (34.5)	2 (1)
<i>P</i> value	0.025**	0.030**	0.070*	0.044**
PR- (<i>n</i> =53)	125.0 (32.5)	31.0 (36.5)	125.0 (30.0)	1 (1)
PR+ (<i>n</i> =92)	109.5 (36.8)	25.0 (25.5)	114.0 (33.8)	2 (1)
<i>P</i> value	0.001**	0.106	0.002**	0.054*
G1 (<i>n</i> =9)	112.0 (29.0)	29.0 (46.0)	119.0 (21.0)	1 (1.5)
G2 (<i>n</i> =44)	113.5 (44.5)	31.5 (34.0)	117.0 (40.5)	1 (1)
G3 (<i>n</i> =92)	113.5 (38.0)	25.0 (30.3)	118.0 (34.0)	1 (1)
<i>P</i> value	0.984	0.343	0.996	0.759

Median values are given with their interquartile ranges (Q75–Q25) in parentheses; significant differences on the 0.05 level are marked by **, on the 0.1 level by *

Abbreviations: LN-, lymph node negative; LN+, lymph node positive; HER-2-, HER-2/neu score 0–2; HER-2+, HER-2/neu score 3; ER-, estrogen receptor positive cells ≤10%; ER+, estrogen receptor positive cells >10%; PR-, progesterone receptor positive cells ≤10%; PR+, progesterone receptor positive cells >10%; IQR, interquartile range

tumours were larger in size (median 1.79, interquartile range 2.81 ccm) compared with HER-2/neu negative tumours (median 0.93, interquartile range 2.7 ccm). A higher volume of plateau voxels was found in HER-2/neu positive cases (median 0.52, interquartile range 1.02 ccm) compared with HER-2/neu negative cases (median 0.23, interquartile range 0.75 ccm).

The other kinetic profile parameters did not display any significant differences between HER-2/neu positive and HER-2/neu negative lesions (cf. Tables 1 and 2).

Binary logistic regression analysis therefore implied that total volume and plateau voxel volume were independent predictors of HER-2/neu status.

Lesion features and oestrogen receptors (ER)

Forty-one lesions expressed ER in ≤10% of all histologically analysed cells, whereas 104 lesions expressed ER in more than 10%. Significant differences between these groups (i.e. higher values in ER negative compared with ER positive cases) were found for colour-coded volume as well as for persistent, plateau and washout voxel volumes ($P < 0.018$, respectively). Strong enhancing voxel volume tended to be higher in ER negative cases ($P = 0.060$, cf. Table 2). Initial enhancement percentage and washout rate were significantly higher in ER negative compared with ER positive cases ($P < 0.030$, cf. Table 1). The time to peak of the most suspect curve was shorter in ER negative cases

($P = 0.044$) and maximum enhancement tended to be higher in ER negative cases ($P = 0.070$, cf. Table 1).

The other dynamic features examined showed no significant differences between ER positive and ER negative lesions (cf. Tables 1 and 2).

Logistic binary regression analysis identified initial enhancement of the most suspect curve, total volume and plateau voxel volume as independent predictors for ER status.

Lesion features and progesterone receptors (PR)

The percentage of PR positive cells was ≤10% in 53 lesions, whereas 92 lesions were PR positive above 10%. By comparing these groups with examined radiological parameters, we found significant differences for strongest initial enhancement ($P = 0.001$), peak enhancement ($P = 0.002$), tumour volume ($P = 0.011$), persistent, plateau and washout volume ($P < 0.026$, respectively; cf. Table 2) as well as for percentage and volume of strong enhancing voxels ($P < 0.017$, respectively; cf. Table 2). Time to peak of the most suspect curve tended to be higher in ER positive tumours ($P = 0.054$, cf. Table 1).

The other kinetic profile parameters did not show significant differences between progesterone receptor positive and progesterone receptor negative lesions (cf. Tables 1 and 2).

After binary logistic regression analysis, initial enhancement of the most suspect curve, total volume as well as

Table 2 Prognostic pathological factors and analysed MRI features

Prognostic factor	Total volume (ccm)	Overall persistent enhancement (median %)	Persistent enhancement volume (ccm)	Overall plateau enhancement (median %)	Plateau enhancement volume (ccm)	Overall washout enhancement (median %)	Washout enhancement volume (ccm)	Overall strong enhancement (median %)	Strong enhancement volume (ccm)
LN ⁻ (n=100)	0.78 (2.6)	44.5 (39.2)	0.31 (0.81)	27.6 (14.8)	0.22 (0.78)	18.5 (37.8)	0.16 (0.90)	8.8 (19.3)	0.08 (0.38)
LN ⁺ (n=45)	1.72 (3.04)	36.0 (37.2)	0.70 (1.77)	31.8 (16.5)	0.51 (1.04)	20.2 (28.2)	0.30 (1.18)	9.2 (18.7)	0.15 (0.70)
P value	0.002**	0.386	0.007**	0.140	0.003**	0.797	0.085*	0.892	0.366
HER-2 ⁻ (n=102)	0.93 (2.7)	41.9 (40.3)	0.36 (0.82)	28.3 (17.0)	0.23 (0.75)	20.9 (37.8)	0.16 (0.89)	8.5 (20.0)	0.08 (0.34)
HER-2 ⁺ (n=43)	1.79 (2.81)	44.5 (34.9)	0.53 (1.16)	27.4 (12.7)	0.52 (1.02)	16.0 (29.9)	0.32 (1.03)	9.7 (15.4)	0.10 (0.49)
P value	0.076*	0.752	0.109	0.612	0.026**	0.803	0.247	0.295	0.172
ER ⁻ (n=41)	1.95 (3.37)	44.1 (32.2)	0.57 (1.04)	27.6 (10.4)	0.61 (0.88)	27.5 (34.3)	0.46 (1.48)	8.9 (20.9)	0.14 (1.02)
ER ⁺ (n=104)	0.90 (2.29)	39.9 (42.9)	0.31 (0.84)	28.3 (17.4)	0.23 (0.64)	15.7 (31.7)	0.15 (0.59)	9.4 (18.2)	0.08 (0.36)
P value	0.015**	0.551	0.016**	0.700	0.018**	0.134	0.011**	0.239	0.060*
PR ⁻ (n=53)	1.95 (3.48)	44.5 (35.8)	0.56 (1.06)	27.4 (11.7)	0.59 (0.98)	25.8 (36.1)	0.41 (1.37)	10.6 (20.9)	0.21 (0.84)
PR ⁺ (n=92)	0.87 (1.87)	39.9 (41.5)	0.29 (0.83)	29.1 (16.4)	0.23 (0.62)	16.0 (29.2)	0.13 (0.59)	7.8 (16.4)	0.06 (0.28)
P value	0.011**	0.584	0.026**	0.577	0.024**	0.259	0.022**	0.017**	0.006**
G1 (n=9)	0.84 (4.76)	33.3 (49.4)	0.23 (3.34)	29.0 (30.0)	0.21 (1.32)	20.5 (46.2)	0.17 (0.88)	12.9 (17.0)	0.14 (0.28)
G2 (n=44)	0.92 (2.65)	33.5 (38.2)	0.29 (0.68)	29.2 (15.5)	0.26 (0.59)	26.5 (37.3)	0.19 (1.57)	12.5 (25.3)	0.08 (0.47)
G3 (n=92)	1.17 (2.72)	47.6 (38.5)	0.50 (1.02)	27.5 (14.2)	0.33 (0.85)	16.2 (30.3)	0.19 (0.89)	7.5 (15.5)	0.10 (0.39)
P value	0.641	0.240	0.330	0.608	0.717	0.411	0.919	0.440	0.972

Median values are given with their interquartile ranges (Q75-Q25) in parentheses; significant differences on the 0.05 level are marked by **, on the 0.1 level by *
Abbreviations: LN⁻, lymph node negative; LN⁺, lymph node positive; HER-2⁻, HER-2/neu score 0-2; HER-2⁺, HER-2/neu score 3; ER⁻, estrogen receptor positive cells ≤10%; ER⁺, estrogen receptor positive cells >10%; PR⁻, progesterone receptor positive cells ≤10%; PR⁺, progesterone receptor positive cells >10%; IQR, interquartile range

Table 3 Binary logistic regression analysis results (backward likelihood ratio selection)

	β (SE)	Odds ratio	95% CI	<i>P</i> value
Lymph node status				
Time to peak	-0.520 (0.210)	0.594	0.394–0.898	0.013
HER-2/neu status				
Total volume	-0.243 (0.124)	0.784	0.615–1.000	0.050
Plateau volume	0.761 (0.428)	2.141	0.925–4.955	0.075
ER status				
Initial enhancement	-0.015 (0.008)	0.985	0.971–1.000	0.054
Total volume	-0.223 (0.125)	0.800	0.626–1.023	0.075
Plateau volume	0.753 (0.444)	2.123	0.889–5.070	0.090
PR status				
Initial enhancement	-0.023 (0.008)	0.977	0.962–0.992	0.003
Total volume	0.668 (0.381)	1.950	0.923–4.117	0.080
Persistent volume	-0.966 (0.548)	0.380	0.13–1.113	0.078
Washout volume	-0.881 (0.507)	0.414	0.153–1.119	0.082

Abbreviations: ER, estrogen receptor; PR, progesterone receptor

persistent and washout voxel volumes remained as independent predictors of PR status.

Lesion features and grading

Histopathology revealed 9 well-differentiated lesions (G1), 44 fairly differentiated lesions (G2) and 92 poorly differentiated lesions (G3).

All examined dynamic features showed no significant differences between different tumour gradings (cf. Tables 1 and 2).

As no significant differences between examined dynamic enhancement parameters and histopathological prognostic factors were observed, binary logistic regression analysis with grading as independent variable was omitted.

Discussion

There is common agreement that certain factors allow an estimation of tumour prognosis in patients with breast cancer [15–17]. Accepted main prognostic factors include occurrence of lymph node metastasis and tumour grading. Breast cancer with high nuclear grade (low differentiation grade) and lymph node infiltration has the poorest prognosis. Further considered prognostic factors are expression level of oestrogen receptors (ER), progesterone receptors (PR) and HER-2/neu receptors; however, their value remains controversial [16–18]. Although patients with ER positive tumours were reported to have prolonged disease-free survival after primary treatment and longer survival after recurrence compared with patients with ER negative tumours [18], it is difficult to exclude the influence of therapy, since ER positive patients receive and benefit from either adjuvant or palliative hormone therapy. The presence of PR is strongly

related to ER receptor status due its expression only after transcriptional activation of its gene by a functional ER–oestrogen complex. High HER-2/neu receptor expression on the other hand was reported to be related to poor prognosis [16, 19], especially in nodal positive patients.

In the current study we correlated the aforementioned prognostic factors with enhancement features on MR mammography. The rationale behind the study design was the following: It is believed, that every growing tumour exceeding a diameter of a few millimetres induces angiogenesis to maintain oxygen and nutriment supply [20]. Furthermore, although controversial, microvessel density (MVD), i.e the grade of neovascularisation of a tumour was reported to correlate with tumour aggressiveness and its potential to metastasize [21]. Since the reason for tumour enhancement in breast MRI is believed to be angiogenesis, we wondered whether the aforementioned correlation is transferable to this imaging modality.

We applied a computer-aided program capable of semi-automatic assessment of kinetic features in a given lesion. The advantage of this approach lies in the exclusion of interobserver variability, as well as additional information on the enhancement pattern distribution of the whole lesion.

Our results show that a shorter time to peak is the only independent parameter associated with nodal positive cases, indicating a more benign enhancement pattern in less aggressive tumours. Previous studies demonstrated a somewhat higher initial enhancement rate in node positive patients compared with node negative patients, a finding which we cannot confirm [10, 12]. However, our results are congruent with other investigations [4, 13]. Furthermore, automatically calculated larger lesion volumes as well as voxel type subvolumes were associated with a higher locoregional metastasis rate. This finding is in agreement with previous publications on tumour size and nodal metastasis [22]. Aside from nodal status, hormone receptor and HER-2/neu status of

invasive carcinomas were significantly influenced by enhancement characteristics in our study. HER-2/neu positive tumours were significantly larger compared with HER-2/neu negative tumours. Further enhancement patterns did not differ between HER-2/neu subgroups. Independent predictors for hormone receptor status were initial enhancement of the most suspect curve as well as tumour volumes. ER/PR negative lesions showed a stronger and faster initial enhancement compared with ER/PR positive lesions. Washout rate of ER negative lesions was higher and ER/PR negative lesions were larger in size. These findings indicate a more aggressive tumour biology. Previous reports on such correlation are varying. A more recent investigation compared MRI features between ER positive and ER negative tumours, and the authors were able to demonstrate a trend of ER negative tumours towards more malignant enhancement kinetics [23]. Other authors either confirmed [24] or failed to find a correlation [4]. Our results corroborate a significant influence of hormone receptor status on MRI enhancement characteristics, reflecting a more aggressive tumour growth pattern. Aggressiveness of such tumours is also underlined by the known higher rate of distant visceral metastases and poorer overall prognosis in ER/PR negative cancers [16, 17, 25]. Dedicated histopathological analysis of hormone receptor positive and negative cases might show whether microvessel density is different among these groups or if a different vessel structure is responsible for the identified enhancement characteristics.

Regarding tumour grade and enhancement pattern, we did not find any significant influence on the enhancement pattern of the examined lesions. Our findings are congruent with previous groups [4, 13]; however, a few other publications reported a correlation—albeit minor—between tumour grade and enhancement curves [10, 12]. A variety of reasons might explain these contradictory findings. With 9 out of 145 lesions (6.2%), G1 cancers represented a small subgroup in our patient collective. Although this proportion is in good agreement with the epidemiological literature [26] and underlines the representativeness of our patient collective, small subgroup differences are possibly missed because of low G1 sample size. In contrast to well-differentiated (G1) breast neoplasms, poorly differentiated G3 cancers have been described as a biologically different disease [27]. Intermediate grade cancers (G2) are a more heterogeneous subgroup showing overlap in biological properties with the other subgroups, especially G3 [27]. This fact is underlined by the

limited reliability to differentiate between these entities by means of histopathological criteria [28]. These reasons might explain missing differences between kinetic enhancement patterns and grading in our study.

There are certain limitations of the current study. Various institutions use different MR scanners, imaging protocols and sequences, complicating comparisons of semiquantitative dynamic parameters between different publications. A study by Pabst et al. [29] on phantoms for example demonstrated that characteristics of contrast enhancement vary significantly depending on the protocol used and, furthermore, even with the same protocol different signal enhancements are obtained depending on the MR scanner. Also, enhancement characteristics are significantly influenced by physiological parameters, such as the arterial input function [30]. These might be major reasons for the varying results concerning enhancement kinetics in the reviewed literature. To obtain tissue microcirculation characteristics in detail, several pharmacokinetic modelling approaches have been used. However, pharmacokinetic analysis of dynamic contrast-enhanced MRI data is a field of ongoing research and resulting parameters strongly depend on the algorithm used, the arterial input function, image noise and the method of contrast agent administration [31]. Because of these limitations and the insufficient temporal resolution of our clinical protocol to reliably perform pharmacokinetic modelling, we omitted this approach and concentrated on a more simple method which is broadly available and has been described previously [14].

A second reason for such variations is probably the fact that evaluation of enhancement kinetics in previous literature was performed by manually placing an ROI in the most enhancing part of the lesion. Consequently, interobserver variations due to individually chosen ROI sizes and ROI placements are likely. Therefore we used an automatic enhancement evaluation program in this study that excluded this probable bias. To our knowledge we were the first to perform such correlation studies using automatic kinetic assessment.

In summary we demonstrated that some kinetic features of invasive breast carcinomas in MRM (i.e. strong initial enhancement, time to peak and higher tumour volumes including subvolumes of different curve types) correlate with nodal, HER-2/neu and hormone receptor status. We conclude that lesions exhibiting a strong initial enhancement, a short time to peak and larger volume are more likely to be associated with poorer prognostic factors than lesions lacking these features.

References

1. Bone B, Aspelin P, Bronge L et al (1996) Sensitivity and specificity of MR mammography with histopathological correlation in 250 breasts. *Acta Radiol* 37:208–213
2. Drew PJ, Chatterjee S, Turnbull LW et al (1999) Dynamic contrast enhanced magnetic resonance imaging of the breast is superior to triple assessment for the pre-operative detection of multifocal breast cancer. *Ann Surg Oncol* 6:599–603
3. Kaiser WA, Zeitler E (1989) MR imaging of the breast: fast imaging sequences with and without Gd-DTPA. Preliminary observations. *Radiology* 170:681–686

4. Stomper PC, Herman S, Klippenstein DL et al (1995) Suspect breast lesions: findings at dynamic gadolinium-enhanced MR imaging correlated with mammographic and pathologic features. *Radiology* 197:387–395
5. Berg WA, Gutierrez L, NessAiver MS et al (2004) Diagnostic accuracy of mammography, clinical examination, US, and MR imaging in preoperative assessment of breast cancer. *Radiology* 233:830–849
6. Fischer DR, Wurdinger S, Boettcher J et al (2005) Further signs in the evaluation of magnetic resonance mammography: a retrospective study. *Invest Radiol* 40:430–435
7. Kaiser WA (2007) Breast magnetic resonance imaging: principles and techniques. *Semin Roentgenol* 42:228–235
8. Malich A, Fischer DR, Wurdinger S et al (2005) Potential MRI interpretation model: differentiation of benign from malignant breast masses. *AJR* 185:964–970
9. Neubauer H, Li M, Kuehne-Heid R et al (2003) High grade and non-high grade ductal carcinoma in situ on dynamic MR mammography: characteristic findings for signal increase and morphological pattern of enhancement. *Br J Radiol* 76:3–12
10. Mussurakis S, Buckley DL, Horsman A (1997) Dynamic MR imaging of invasive breast cancer: correlation with tumour grade and other histological factors. *Br J Radiol* 70:446–451
11. Narisada H, Aoki T, Sasaguri T et al (2006) Correlation between numeric gadolinium-enhanced dynamic MRI ratios and prognostic factors and histologic type of breast carcinoma. *AJR* 187:297–306
12. Tuncbilek N, Karakas HM, Okten OO (2005) Dynamic magnetic resonance imaging in determining histopathological prognostic factors of invasive breast cancers. *Eur J Radiol* 53:199–205
13. Fischer U, Kopka L, Brinck U et al (1997) Prognostic value of contrast-enhanced MR mammography in patients with breast cancer. *Eur Radiol* 7:1002–1005
14. Baltzer PA, Renz DM, Kullnig PE et al (2009) Application of computer-aided diagnosis (CAD) in MR-mammography (MRM): do we really need whole lesion time curve distribution analysis? *Acad Radiol* 16:435–442
15. Contesso G, Mouriesse H, Friedman S et al (1987) The importance of histologic grade in long-term prognosis of breast cancer: a study of 1,010 patients, uniformly treated at the Institut Gustave-Roussy. *J Clin Oncol* 5:1378–1386
16. Donegan WL (1997) Tumour-related prognostic factors for breast cancer. *CA Cancer J Clin* 47:28–51
17. Fisher B, Redmond C, Fisher ER et al (1988) Relative worth of oestrogen or progesterone receptor and pathologic characteristics of differentiation as indicators of prognosis in node negative breast cancer patients: findings from National Surgical Adjuvant Breast and Bowel Project Protocol B-06. *J Clin Oncol* 6:1076–1087
18. Stewart JF, Rubens RD, Millis RR et al (1983) Steroid receptors and prognosis in operable (stage I and II) breast cancer. *Eur J Cancer Clin Oncol* 19:1381–1387
19. Marks JR, Humphrey PA, Wu K et al (1994) Overexpression of p53 and HER-2/neu proteins as prognostic markers in early stage breast cancer. *Ann Surg* 219:332–341
20. Folkman J (1971) Tumour angiogenesis: therapeutic implications. *New Engl J Med* 285:1182–1186
21. Weidner N, Semple JP, Welch WR et al (1991) Tumour angiogenesis and metastasis-correlation in invasive breast carcinoma. *New Engl J Med* 324:1–8
22. Tresserra F, Rodriguez I, Garcia-Yuste M et al (2007) Tumour size and lymph node status in multifocal breast cancer. *Breast J* 13:68–71
23. Chen JH, Baek HM, Nalcioglu O et al (2008) Oestrogen receptor and breast MR imaging features: a correlation study. *J Magn Reson Imaging* 27:825–833
24. Szabo BK, Aspelin P, Kristoffersen Wiberg M et al (2003) Invasive breast cancer: correlation of dynamic MR features with prognostic factors. *Eur Radiol* 13:2425–2435
25. Dent R, Hanna WM, Trudeau M et al (2009) Pattern of metastatic spread in triple-negative breast cancer. *Breast Cancer Res Treat* 115:423–428
26. Henson DE, Chu KC, Levine PH (2003) Histologic grade, stage, and survival in breast carcinoma: comparison of African American and Caucasian women. *Cancer* 98:908–917
27. Ignatiadis M, Sotiriou C (2008) Understanding the molecular basis of histologic grade. *Pathobiology* 75:104–111
28. Longacre TA, Ennis M, Quenneville LA et al (2006) Interobserver agreement and reproducibility in classification of invasive breast carcinoma: an NCI breast cancer family registry study. *Mod Pathol* 19:195–207
29. Pabst T, Kenn W, Kaiser WA et al (2001) Understanding why contrast enhancement in dynamic MRI is not reproducible: illustration with a simple phantom. *Breast J* 7:166–170
30. Port RE, Knopp MV, Brix G (2001) Dynamic contrast-enhanced MRI using Gd-DTPA: interindividual variability of the arterial input function and consequences for the assessment of kinetics in tumours. *Magn Reson Med* 45:1030–1038
31. Zwick S, Brix G, Tofts PS et al (2009) Simulation-based comparison of two approaches frequently used for dynamic contrast-enhanced MRI. *Eur Radiol*. doi:10.1007/s00330-009-1556-6